Quantitative Coronary Arteriography

Estimation of Dimensions, Hemodynamic Resistance, and Atheroma Mass of Coronary Artery Lesions Using the Arteriogram and Digital Computation

B. GREG BROWN, M.D., PH.D., EDWARD BOLSON, M.S., MORRIS FRIMER, M.S.E., AND HAROLD T. DODGE, M.D.

SUMMARY **More accurate characterization of coronary artery lesions is needed for evaluation of short and long-term interventions in coronary disease. A method of segmental artery analysis has been developed to maximize the information obtained from coronary arteriograms. Coronary lesions are traced from two projected, perpendicular, 35 mm cineangiographic views and transmitted, in digital form, to a PDP 11/45 computer. Magnification and distortion of the image are compensated for in order to determine the actual vessel profiles, using the catheter and its location as a scaling device. The two views are matched; a spatial representation of the vessel centerline is constructed mathematically; and orthogonal vessel diameters are computed at increments along this centerline. Assuming an elliptical lumen, the absolute and percentage reduction in diameter and cross-sectional area in the stenosis are computed. More complex functions (integrated atheroma mass, Poiseuille resistance, and orifice resistance) are then calculated.**

The accuracy and variability of the different steps involved in lesion analysis have been determined. Dimensional accuracies of ± 150 microns (SD) are feasible. Examples are given of patients with Prinzmetal's angina and with progressive coronary disease.

VISUAL INSPECTION OF CORONARY ARTERIOGRAMS traditionally has been used to assess the clinical severity of coronary disease. However, a more precise method of lesion characterization is needed if we are to evaluate pharmacologic and dietary interventions in coronary atherosclerosis. Previous reports have focused on the difficulties of developing a precise methodology.[1-7]

Robbins et al.[1, 2] tested the usefulness of three methods (angiograms, plastic casts, and opened vessels) in judging the location and severity of arterial lesions in injected postmortem hearts. Although they concluded that the angiographic interpretation was the most consistent, four observers were unable to agree more than 50–70% of the time, even under these ideal circumstances. The same large intra and interobserver variability has been reported for subjective interpretation of clinical coronary cineangiograms.[3]

There are also *theoretical* objections to the traditional "percent stenosis" representation. 1) The hemodynamic effect of coronary artery narrowing is determined by the *absolute* (not *relative*) diameter and also by the length of the stenotic segment. 2) The diseased lumen is commonly eccentric in cross-section, so that a single percent stenosis estimate may not be meaningful.

Methods have been reported for analysis of single angiographic projections using digital computation. Blankenhorn and associates[4, 5] have developed a potentially useful method for detecting the presence of intimal fibrous plaques. They measure vessel lumen irregularity using edge detection by scanning densitometry and computerized curve fitting. The computed irregularity correlates well with vessel surface involvement by early atherosclerotic plaques, and with mural cholesterol concentration in early peripheral vascular disease. However, this method is unsuccessful in characterizing advanced atherosclerotic lesions of the type which result in clinical symptoms; and it does not generate hemodynamic information.

Gensini et al.[6] used digital computation to evaluate vasomobility from coronary cineangiograms. These authors provide an optimistic view: "the image intensifier offers a wealth of data which is, at present, only partially used and seldom *measured* in clinical practice." They claim that vessel diameter estimates were accurate to within less than ± 80 microns (less than ± 3% variability on a typical diameter estimate). However, Crawford et al.[5] point out that the ability to define the lumen edge depends strongly on the intraluminal concentration of contrast medium. They express concern that complex geometry, motion, small arterial size, and contrast dilution make the estimate[6] of ± 80 microns accuracy overly optimistic in coronary lumen edge detection. They do agree with Chilvers et al.[7] that sufficiently precise dimensional estimates may be made from clinical aorta-iliac angiograms.

This report describes an objective method for analysis of a diseased coronary arterial segment. It represents a significant improvement over those methods described above because: 1) it deals at a fundamental level with the magnification and distortion inherent in cineangiography; 2) it uses perpendicular cine projections to construct a 3-dimensional, true-scale representation of the diseased arterial segment; and 3) it computes other potentially important parameters of lesion severity.

The precision of the method is evaluated and examples of its clinical applications are given.

Methods

Clinical coronary cineangiograms are obtained in routine fashion in multiple single-plane projections. For each projection in the LAO, a complementary projection at 90° is obtained in the RAO. For example, a complementary pair might be 60° LAO and 30° RAO.

From the Cardiology Divisions, University of Washington, School of Medicine, Seattle, Washington; and Wadsworth Veterans Administration Hospital, Los Angeles, California.

Supported in part by USPHS Grants HL 13517, HL 19451 and HL 18805, by VA Project 1102-01, by the Poncin Research Fund, and by the Safeco Fellowship Fund.

Address for reprints: B. G. Brown, M.D., Cardiology Division, Wadsworth Veterans Administration Hospital, Wilshire and Sawtelle Boulevards, Los Angeles, California 90073.

The radiographic equipment is of Philips manufacture with an X-ray tube and cesium iodide 9/5 inch image intensifier mounted on a vibration-free Picker c-arm assembly at 81.3 cm focal spot/input surface distance. The focal spot size for cine radiography is 0.6 cm^2 and the image tube operated in 9 inch and 5 inch mode with 100 mm overframing cine camera lens for the images reported here. X-ray exposure time is 5 msec, 80–85 kV and 300 mA. Films are made at 30 frames per second on 35 mm Kodak Shellburst 5474 gray base film with an Arriflex camera. Carefully controlled film processing results in high contrast images. Any equipment of comparable resolution would be suitable.

Selected cine frames are projected by a Vanguard Model M-35C projector onto a 52 × 67 cm screen. The screen is marked off in rectilinear (x, y) coordinates, with the (0, 0) point at its center. In the derivations that follow, three coordinate systems will be employed, as shown in figure 1. They all have the same orientation, but differ in scale.

XR, YR; XL, YL are the (x, y) coordinates in the plane of the projected image in the RAO and LAO views, respectively. YR and YL fall along a common axis roughly corresponding to the patient long axis, and XR and XL are axes perpendicular to the Y axes and to each other.

X'R, Y'R; X'L, Y'L are the coordinates in the respective image planes from which the effects of pincushion distortion have been mathematically eliminated.

xr, yr; xl, yl are the true-scale coordinates in each view.

The selected arterial segment and a portion of the catheter, of known dimension, near its tip are traced from the projected view and from the complementary view at 90°. Although the two projections were *not* filmed simultaneously, each of the two complementary images was traced at approximately the same point in the cardiac cycle, e.g., end systole, end diastole, or mid-cycle. The X, Y coordinates of the mid-point, C, of the traced catheter segment and of a reference point, P, on the lesion are specified as numerical input data. P is usually selected as the mid-point of the lesion at its narrowest diameter; or it may be specified as a branch point, or a bit of mural calcium seen in each view.

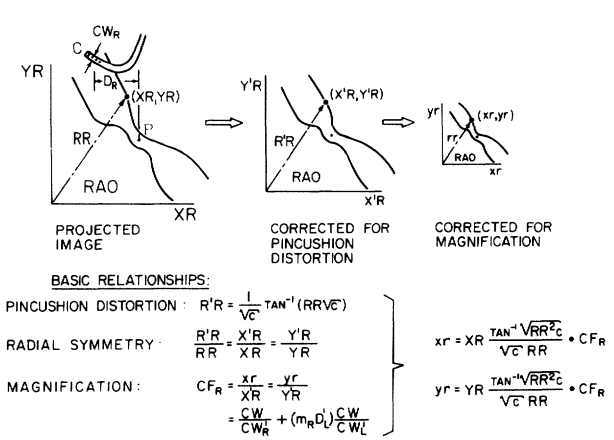

FIGURE 1. *Illustration of the three different coordinate systems employed in lesion analysis. On the left is the image plane of the projected cine frame, with X, Y coordinates centered in the frame. The projected image is corrected first for pincushion distortion and then for magnification to arrive at a true-scale representation of the traced vessel image. The expressions given below define the mathematical relationships among the coordinate systems, and are more fully explained in the text.*

The traced vessel segments are converted to digital form by means of an Autotrol 3400-B digitizer with a resolution of 0.1 mm, and transmitted to the PDP 11/45 computer operating under the multitask operating system RSX 11-D containing the task "artery." Visual interaction with the computer is done using a Tektronics 4012 terminal. Thus the two borders of the traced vessel segment in RAO are characterized as a series of points $(XR, YR)_m$ and in LAO as a series of points $(XL, YL)_n$. This coordinate representation is transformed by two correction processes to the true-scale representation of the arterial segment.

Pincushion Correction

Pincushion distortion results from the convex curvature of the input phosphor vacuum tube. This results in selective magnification of an object near the edges of the cine frame compared to its size in the center of the field. If pincushion effect is present cinematography of the rectilinear grid will result in a distorted rectilinear image, as illustrated in figure 2a. This effect is more pronounced when larger areas of the input phosphor are used for image production as seen in figure 2b. The pincushion effect is theoretically radially symmetric about the central X-ray beam; this depends on the rotational symmetry of the curved input phosphor tube and its internal fields. For practical purposes, we have assumed and confirmed that the pincushion effect is radially symmetric, and have empirically determined an analytic function of radius which characterizes the distortion. Without justifying the results on theoretical grounds, we found that the following expression fits the data well (see data of fig. 2b).

$$\Delta R' = \frac{\Delta R}{(1 + cR^2)} \qquad 1.$$

Where: R is the radial distance from the center of the screen to a projected image point.

ΔR is the measured interval between two adjacent lines of a 1 cm grid, when the latter is filmed and projected on the screen.

$\Delta R'$ is the grid interval that would be measured in the absence of pincushion distortion. In practice it is the grid-line interval at the center of the screen, ΔRo, where pincushion effect is negligible.

c is an empirically determined coefficient, 5.0×10^{-4} cm^{-2} in the standard 10 inch view, and 1.25×10^{-4} cm^{-2} in the 6 inch view.

The following integral relationship exists between radial dimensions in these two coordinate systems:

$$\int_0^{R'} dR' = \int_0^{R} \frac{dR}{1 + cR^2} \qquad 2.$$

where dR' and dR represent the limiting incremental values of $\Delta R'$ and ΔR. Carrying out the integration gives:

$$R' = \frac{1}{\sqrt{c}} \tan^{-1}(R\sqrt{c}) \qquad 3.$$

The following algebraic transformations, together with expression 3. are used to convert the sets of points of the

digitized images, $(XR, YR)_m$ and $(XL, YL)_n$, to the corresponding sets of points in pincushion-free coordinates:

$$X' = (R'/R)\ X$$
$$Y' = (R'/R)\ Y \qquad 4.$$

Magnification Correction

Once the magnified arterial segment is traced and digitized, and pincushion distortion is mathematically eliminated, residual magnification is compensated to reduce the images to their true scale. A *correction factor,* CF, is determined for each view such that the product (CF × projected dimension) gives the actual dimension. The correction factors accomplish the second coordinate transformation of figure 1, and are defined by the following expressions:

$$CF_R = \frac{CW}{CW_R'} + (m_R\ D_L')\ \frac{CW}{CW_L'}$$
$$CF_L = \frac{CW}{CW_L'} + (m_L\ D_R')\ \frac{CW}{CW_R'} \qquad 5.$$

where: CF_R, CF_L are the correction factors in the respective RAO and LAO views, defined such that a projected dimension in that view (already corrected for pincushion distortion) is reduced to its true dimension when multiplied by CF.

CW is the known catheter diameter at its point of measurement.

CW_R', CW_L' are the dimensions of the traced catheter segments in their respective views. The prime (′) reflects that these dimensions have been corrected for pincushion distortion.

D_R', D_L' are horizontal distances separating the lesion center P, and the traced catheter segment, C, in the respective views. See figure 1. Again, the prime (′) reflects that these distances have been corrected for pincushion distortion.

m_R, m_L are coefficients characteristic of the X-ray system, and are defined as the rate of change of the correction factor with distance along the axis of the divergent X-ray beam. m_R and m_L are -0.0037 and $+0.0037$ cm^{-1}, respectively, in the 9 inch angiographic mode, and -0.0020 and $+0.0020$ cm^{-1} in the 5 inch mode.

The initial terms (CW/CW_R') in the correction factor expressions simply state that the catheter tip is used as a scaling device. The beam divergence terms containing m_R and m_L permit a first-order correction for differential magnification resulting from separation of the arterial lesion and catheter tip along the beam axis. Thus, as illustrated in figure 1, the sets of points $(X'R, Y'R)_m$ and $(X'L, Y'L)_n$ defining the traced arterial segment corrected for pincushion distortion are converted to true scale $(xr, yr)_m$ and $(xl, yl)_n$ by multiplying the coordinates of each point by the appropriate correction factor.

Centerline

As shown in the panels of figure 3, the traced vessel segment may be characterized as a series of lumen diameters distributed along the centerline of the segment. The centerline is mathematically defined such that its perpendicular at any point intersects both vessel edges at equal distances from itself. Sets of points $(xr, yr)_p$ and $(xl, yl)_q$ describing the centerline in each view are computed, together with the corresponding sets of projected diameters $(dr)_p$ and $(dl)_q$.

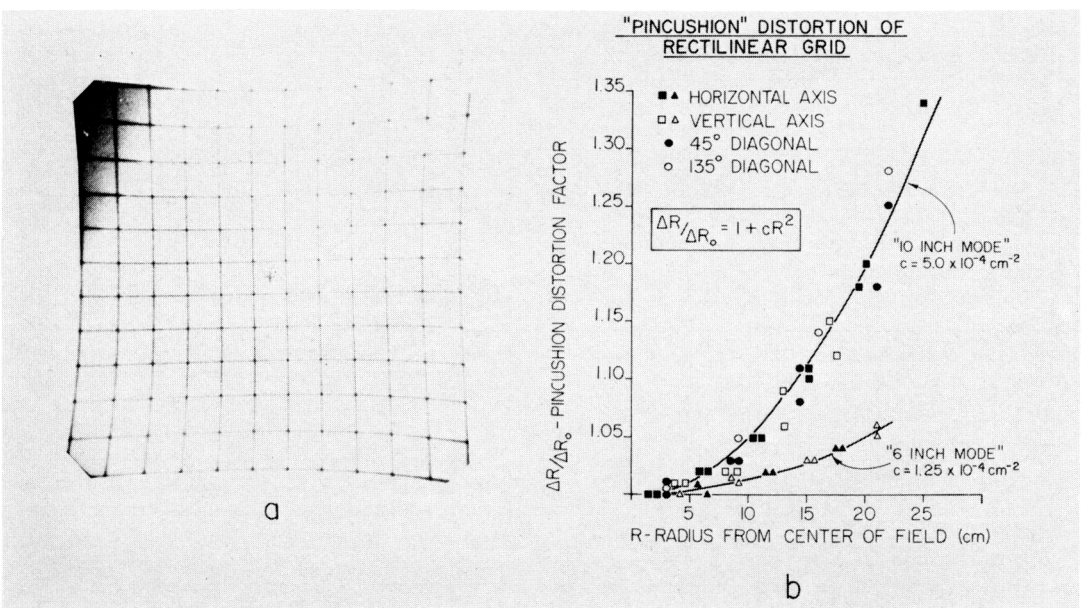

FIGURE 2. *a) Pincushion distortion is illustrated in this cine frame of a rectilinear grid with 1 cm spacing. Objects in the periphery of the angiographic field are selectively magnified relative to their size in the center of the field. b) The relative magnification occurring with pincushion distortion can be empirically characterized by a function whose value is unity at the center of the field and proportional to* $(1 + cR^2)$ *at points a radial distance, R, away from the center.* ΔR *is the grid interval at a point, R, in the field;* ΔR_o *is the interval at the center. Radial symmetry is demonstrated by the similarity of results determined along different axes. Distortion is much less striking when the magnified 6 inch angiographic mode is employed. These are constants determined for the General Electric Flouricon 300 System used at the Wadsworth VA Hospital.*

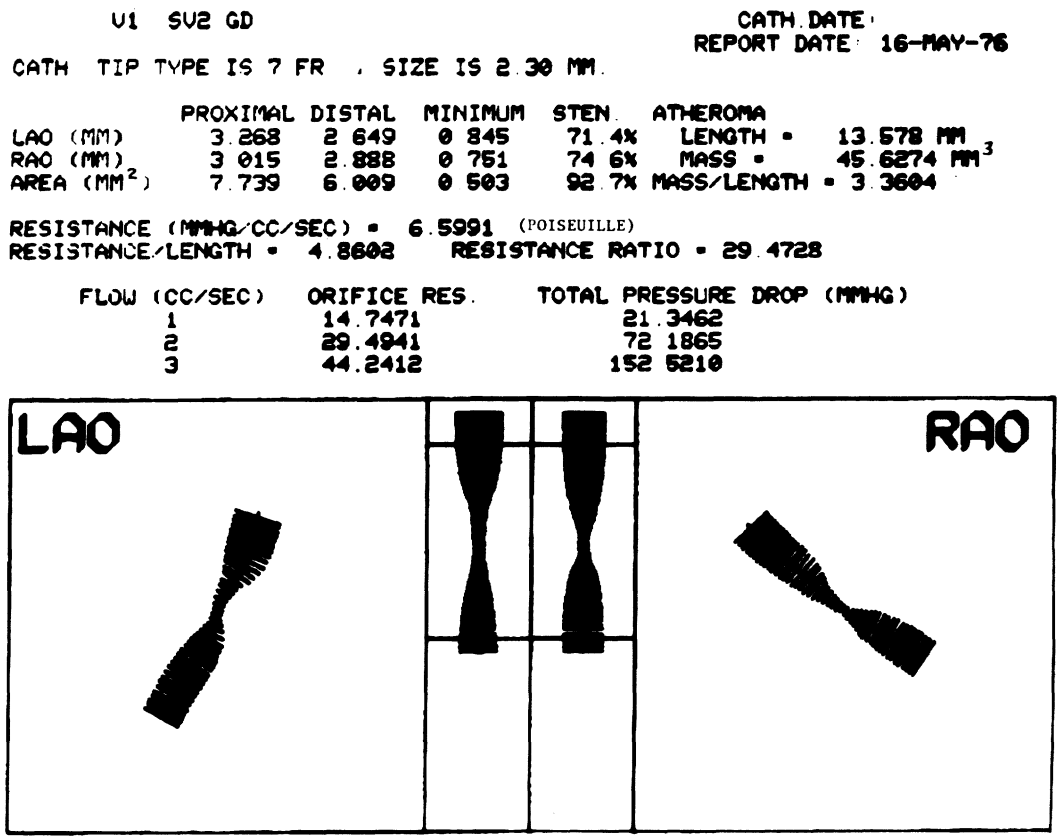

FIGURE 3. *Example of the hard copy printout of segmental analysis of a coronary artery lesion. The lesions are portrayed to scale in the outer boxes, with a scale dimension of 3 cm along the box edge. The inner panels show matched portions of the two views stretched out to true length at the same scale. The computations are explained in the text.*

This useful representation permits the combination of data from the two projected views to yield a three-dimensional characterization of the vessel segment. The two views are first matched at a point thought to be identical in both. This might be a vessel branch point, a bit of mural calcium, or the point of maximum lumen constriction. The two views are approximately matched initially through the estimated centerpoints, P, specified as input data. The computer refines this approximation by searching about P for $\pm$ 0.2 mm along the centerline to find the minimum local diameter in each view. The centerline points corresponding to these minimum diameters are then redefined as 0, 0 for the sets of points $(xr, yr)_p$ and $(xl, yl)_q$. Thus we have chosen arbitrarily to match the two views of the vessel segment at points of minimum lumen diameter near the estimated matching points in each view.

Since the y-axis is common to the two views, which are reduced to true scale with a matched origin, centerline points having equal y-values in the two views are, by definition, identical. Using this fact, the two projected centerlines are matched along their entire length to construct a three-dimensional centerline composed of the points $(xr, xl, y)_i$ under a unified subscript, i, with corresponding vessel diameters dr_i and dl_i. This is done by a repetitive incremental process of linear interpolation between the established values of the centerline points and of the diameters characterizing the two views.

A new centerline coordinate, s, is defined as distance from the origin along this three dimensional centerline:

$$s_i = \sum_{j=1}^{i} (\Delta xr_j^2 + \Delta xl_j^2 + \Delta y_j^2)^{1/2} \qquad 6.$$

The desired result is a representation of the arterial segment as paired diameters, dr_i and dl_i, corresponding to the centerline coordinate, s_i. The two views are now fully matched along the three dimensional centerline, and may be "stretched out" to true length, side-by-side, as illustrated in the center panels of figure 3.

Although atherosclerotic lesions are not necessarily axially symmetric, the proposed calculations are independent of the eccentricity of the lesion; so for purposes of simplification, the idealized projections of figure 3 are axially symmetric.

Lesion Computations

Length. These idealized, matched views of the vessel segment are displayed on the screen of the Tektronics 4012 terminal. The operator defines the extent of the lesion by moving a cursor (visible horizontal line) on the screen to the "normal proximal" portion of the vessel just above the constriction, and then to the "normal distal" portion just below the constriction. Refer to the center panels of figure 3. This identifies, for the computer, values of the subscript i at which the lesion is said to begin ($i = \alpha$), and end ($i = \omega$). The length of the lesion is then:

$$s = s_\alpha - s_\omega \qquad 7.$$

Dimensions. The computer thus identifies "normal" vessel diameters proximal and distal to the lesion, in each view. It searches between $i = \alpha$ and ω for the minimum diameter (d_{min}) in each view, to calculate a minimum diameter ratio as:

$$\text{min diam ratio}_{RAO} = \frac{2dr_{min}}{dr_\alpha + dr_\omega} \quad 8.$$

with a similar calculation in the LAO.

Area. Assuming an elliptical vessel cross-section, a set of lumen areas is computed based on the formula:

$$A_i = \frac{\pi (dr_i \cdot dl_i)}{4} \quad 9.$$

The minimum cross-sectional area (A_i min) between $i = \alpha$ and ω is identified by computer search, and the minimum area ratio is computed:

$$\text{min area ratio} = \frac{2A_{i\ min}}{A_\alpha + A_\omega} \quad 10.$$

Atheroma Mass. It is assumed that if the vessel segment were not diseased, its area would taper linearly between A_α and A_ω. The portion of the vessel cross-section which is occupied by atheromatous tissue at a given point would thus be the difference between the measured lumen area and the interpolated "normal" area. The volume or mass of the atheroma may be estimated by a Simpson's rule integral of this difference over the length of the lesion:

$$\text{mass} = \frac{A_\alpha + A_\omega}{2} \cdot s - \sum_{i=\alpha+1}^{\omega} A_i\ (s_i - s_{i-1}) \quad 11.$$

Segmental Resistance. Once the inner lumen of the vessel is characterized in a 3-dimensional fashion, it becomes possible to estimate the hemodynamic effect of the stenosis. Segmental resistance may be estimated, and from this, pressure drops predicted for a range of hypothetical flow rates. Unfortunately, our understanding of the complex geometric factors determining hemodynamic resistance is insufficient to make precise estimates. Recent work by a number of investigators,[8-15] particularly that of Logan[15] has provided information sufficient to generate a conceptual model of the important energy-dissipating processes in an arterial stenosis. The physical model to be described below is largely in accord with the work of these investigators, and is based on the following assumptions (each of which is necessary to make the problem theoretically tractable):

1) Flow in the "normal proximal" portion of the lesion and up to the point of maximal narrowing is assumed *laminar.* This is a reasonable assumption since Reynolds number, Re, in normal arteries is of the order 80–170,[16] well below the critical value of 2000 at which turbulence is likely to develop.
2) Flow in the "normal proximal" portion of the lesion and up to the point of maximal narrowing is assumed *fully developed.* This is probably not strictly true, since the inlet length, $L_i = (0.03\ Re)\ d$, the distance necessary for a flat flow profile to adopt its eventual stable velocity distribution, is of the order 3 tube diameters, d, at Re = 100 and 30 diameters at Re = 1000.[17] Since the length of vascular constrictions ranges between 4 and 20 local diameters, the parabolic profile is likely to be only partially developed in the constriction.
3) Flow is assumed to *separate* from the streamline contours defined by the borders of the arterial lumen in the divergent portion of the stenotic segment whenever the divergence half-angle exceeds 15°. This assumption is based on the studies of Chaturvedi[18] in machined tubes. While the 15° separation threshold pertains strictly to the abrupt angles present in machined tubes, the majority of significant coronary lesions encountered have exit half-angles exceeding 15°. Flow separation generates a local form of turbulence which does not perpetuate itself. Large scale eddies form in the divergent portion of the lesion. Much of the energy of the decelerating fluid is transmitted to these eddies and is subsequently dissipated by viscous processes.

The theoretical expressions for the Poiseuille (R_p) and turbulent (R_t) contributions to flow resistance in the lesion, based on the above conceptual model, are:

$$R_p = 15 \sum_{i=\alpha}^{\omega} \frac{\mu (dr_i^2 + dl_i^2)}{(dr_i^3)(dl_i^3)} (s_i - s_{i-1}) \quad 13.$$

$$R_t = \frac{\rho Q}{0.266} \left(\frac{\phi_{min}}{A_{min}^2} - \frac{\phi_\omega}{A^2_\omega} \right) \quad 14.$$

$$\Delta P = Q (R_p + R_t) \quad 15.$$

Where: Q is mean coronary flow [cm^3/sec].

ρ is fluid density [gm/cm^3] approximately 1.0.

μ is fluid viscosity [gm/cm-sec] approximately .03.[19]

s_i is distance along the three-dimensional centerline [mm].

dr_i, dl_i are perpendicular vessel diameters [mm] at the point s_i.

A_{min}, A_ω are cross-sectional lumen areas at the minimum point, and at the "normal" downstream portion of the lesion [mm^2].

ϕ_{min}, ϕ_ω are functions whose values are to be determined empirically. Their approximate value is 1.0. They cover such indeterminate phenomena as the exact cross-sectional velocity profile, the exact location of the point of separation, and possible contraction of the fluid jet.

ΔP is the predicted pressure drop across a lesion in the presence of a given flow, Q.

Results

Measurement of Known Objects

A dummy arterial segment was machined in brass with a normal diameter of 3.00 mm having a 1.00 cm long "lesion" of uniform 1.50 mm diameter. Cineangiograms were made with a Sones catheter tip, 5.5 Fr, as the scaling device. On repeated measurement, the computed dimensional estimates were exact to within 80 microns of the known value, thus confirming the validity of expressions 1. through 10.

Measurements in Injected Human Coronaries

A blinded study was done to compare computerized angiographic dimensional estimates with those made independently by histopathologic techniques. Diseased arteries were removed from three postmortem human hearts after injection at 100 mm Hg pressure with contrast-

containing gelatin.[20] Angiographic views of these vessels were made in two perpendicular projections; a metal rod of known diameter was included as a scaling device. Referring to these angiograms, certain vessel points were selected from which histologic sections were cut and prepared in routine fashion following formalin fixation. Pre and postfixation gross measurements excluded significant tissue shrinkage. The contrast-filled arterial lumen of the sections was planimetered independently by a pathologist to determine lumen cross-sectional area. The angiographic views of the selected segments were projected onto a screen, traced, and analyzed by the computer method over the short segment from which the histologic section had been taken. Due to uncertainty regarding the exact location of this section in the irregular arterial lumen segment, maximum and minimum lumen areas were determined, providing a range of possible values. Segments with relatively uniform diameters were usually selected to minimize this range. Figure 4 demonstrates the excellent correlation between the computer-predicted range of lumen areas and the value determined independently by planimetry.

It is of interest that the lumen of these pressure-injected specimens appeared quite elliptical in section, and had an average computed major-minor axis ratio of 1.20 ± 0.24. Thus the technique and related assumptions appear to be validated in human pathologic material.

Repeatability. The different steps involved in lesion analysis have been evaluated using a number of representative lesions of 40%–70% diameter reduction. Table 1 summarizes the observed variability, expressed as the standard deviation from the mean value of each estimate, in absolute dimensions and as a percentage of the estimate. See table 1 for statistical definitions. Variability of the estimate was determined for the following cases: 1) Repeated digitizing × 10 of the same pair of traced lesion images. 2) Repeated *tracing* and *digitizing* × 10, by a given person, of a lesion from the same pair of angiographic frames. 3) Repeated tracing and digitizing of a given lesion in three pairs of *end-diastolic* angiographic frames from each of *three successive cardiac cycles* visualized during a given pair of contrast injections. 4) Repeated tracing and digitizing of 10 pairs of angiographic frames equally *spaced throughout the cardiac cycle.* 5) Repeated tracing × 2, by *five totally untrained observers,* of the same pair of angiographic frames. 6) Eight different left anterior descending coronary lesions were analyzed from eight patients with the clinical syndrome of unstable angina. Each lesion was analyzed in three different frame pairs spaced throughout the cardiac cycle by *three observers trained in this method.* Thus each lesion was analyzed nine times. The reported results represent the average variability of the method among these eight lesions.

The angiographic frames selected were representative of the quality that we obtain routinely. Variability was determined using the standard 9 inch angiographic mode and the optional 5 inch magnified mode. As table 1 shows, the variability of the estimates was quite acceptable in most cases. The mechanics of digitizing introduces errors of the order of ± 30 microns. A trained observer can repeatedly process a given lesion to within ± 60–85 microns accuracy, being somewhat more accurate in the 5 inch mode. The variabilities using serial frames in one cardiac cycle, serial end-diastolic frames, five untrained observers, and three trained observers were ± 131, ± 194, ± 280 and ± 100 microns, respectively. In each of these cases, the standard deviation of the *percent stenosis* estimate was less than 5%.

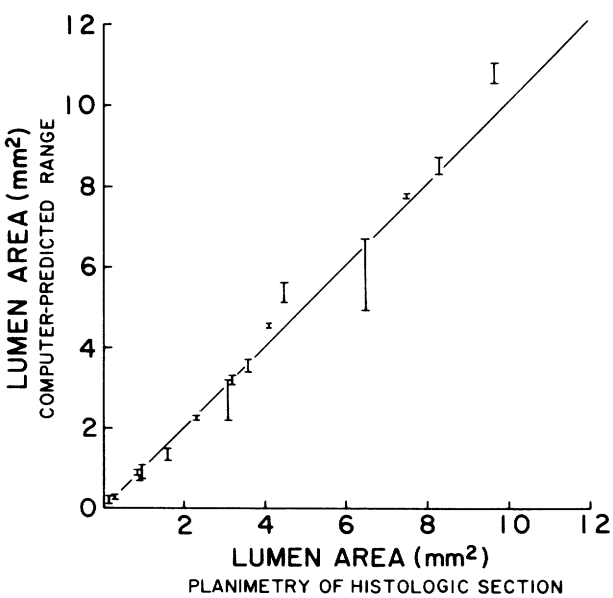

FIGURE 4. *Blinded comparison of computer and histologic measurements of vessel cross-sectional area in contrast-injected postmortem coronary arteries. Using angiograms of the injected vessels, the computer predicted a range of lumen areas for the short vessel segment from when the histologic section was cut. Independent planimetry of the histologic area correlates very well with the computer predictions.*

Clinical Applications

Prinzmetal's Angina

A 56-year-old Caucasian male presented with an 18 month history of classical variant angina[21] of progressive severity. A lateral myocardial infarction had been well documented four months previously. At catheterization, the left coronary artery was selectively visualized to show a 50% stenosis in the mid-left circumflex artery. Without apparent provocation the patient developed typical chest pain. The left coronary artery was re-injected then, and again following relief with nitroglycerin. The computer analysis of the diseased coronary artery segment during these events is shown in figure 5. Chest pain was clearly associated with *diffuse* arterial spasm in the LCCA. The changes of diameter, cross-sectional area, and Poiseuille resistance during spasm, and their reversal by nitroglycerin are documented in figure 5. These observations in a patient with Prinzmetal's angina illustrate the diffuse nature of the vasospasm and demonstrate that such spasm, when associated with moderate atherosclerotic luminal narrowing, can change a modest lesion into a hemodynamically severe one.

Progressive Atherosclerosis

A 43-year-old Caucasian male with stable angina was followed medically for 15 months after coronary arteriography. He then returned with crescendo angina and arteriography was repeated. Five stenotic areas were identified in both studies, and were analyzed by the computer

TABLE 1. *Sources of Variability in Computation Methods*

Steps tested for variability	Lesion	Angio mode	SD† of min. dia. estimate (microns)	SD† of % stenosis estimate (%)	SD† of min. area estimate mm² (% of estimate)	SD† of length estimate mm (% of estimate)	SD† of mass estimate mm³ (% of estimate)	SD† of resistance estimate mm Hg- sec/cm³ (% of estimate)
(1) Repeat (N = 10) digitizing only	56% LCCA	9 inch 5 inch	30 27	1.1% 0.9%	.063% (3.5%) .044 (2.5%)	.32 (3.1%) .41 (4.0%)	1.66 (6.2%) .88 (3.3%)	.051 (5.0%) .036 (3.5%)
(2) Repeat (N = 10) tracing and digitizing, one trained observer	56% LCCA	9 inch 5 inch	84 58	3.8% 1.8%	.180 (10%) .090 (5.1%)	1.00 (9.8%) .53 (5.2%)	7.50 (28%) 1.73 (6.4%)	.11 (11%) .075 (7.3%)
(3) Repeat (N = 10) through one cardiac cycle	50% RCA	9 inch	131	4.9%	.330 (7.7%)	1.56 (5.2%)	23.0 (31%)	.021 (11%)
(4) Repeat (N = 9) serial end-diastolic frames	50% RCA	9 inch	194	4.5%	.560 (13%)	.70 (2.3%)	19.8 (27%)	.036 (18%)
(5) Five totally untrained observers (2x each; N = 10)	38% RCA	9 inch	280	4.2%	.820 (17%)	1.10 (9.0%)	17.90 (31%)	.07 (32%)
(6) Three trained observers, three frames each (N = 9)	68%* LAD	5 inch	100	3.0%	.120 (17%)	1.48 (10.5%)	11.3 (24%)	1.15 (24%)

*Averaged values for 8 different LAD lesions, each analyzed 9 times, i.e., $\overline{SD}(X) = \frac{1}{8}\sum_{i=1}^{8} SD_i(X)$

†$SD(X) = \sqrt{\frac{\sum_i (Xi-\bar{X})^2}{n-1}}$

method. The results of this analysis are summarized in figure 6. There were no interval changes in the so-called normal lumen cross-sectional areas proximal and distal to the stenoses. A previously narrowed segment of the left circumflex artery had become completely occluded. In addition, small but significant area reductions occurred in two other lesions which had appeared unchanged on visual inspection. There was significant progression of computed Poiseuille resistance in four of the five lesions. Cross-sectional area and hemodynamic resistance were relatively stable measurements when three determinations spaced throughout the cardiac cycle were averaged. The resistance appeared to be the more sensitive index of progression. Atheroma mass determinations were quite variable through the cardiac cycle and thus less sensitive indicators of disease progression.

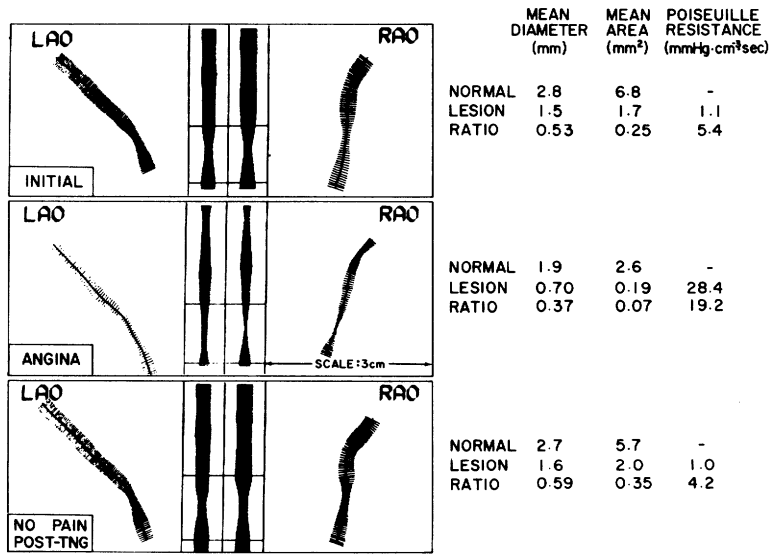

FIGURE 5. *Changes in the dimensions and hemodynamic resistance in the left circumflex coronary artery of a patient with classic Prinzmetal's angina who developed pain and severe spasm in the circumflex and right coronary arteries during catheterization. The pre-existing lesion is between the two horizontal lines in the middle panels, which define the so-called normal proximal and distal ends of the segment. During chest pain, there was diffuse spasm along the entire proximal and mid-portions of the vessel. The previously "normal" portions of the vessel constricted to 40% of the original cross-sectional area; in the lesion, cross-section was 11% of the pre-pain value, and Poiseuille resistance increased 26-fold. Nitroglycerin completely reversed the spasm, but did not eliminate the fixed stenosis. This observation suggests that diffuse arterial spasm in association with a modest atheromatous lesion can result in transient severe flow limitation.*

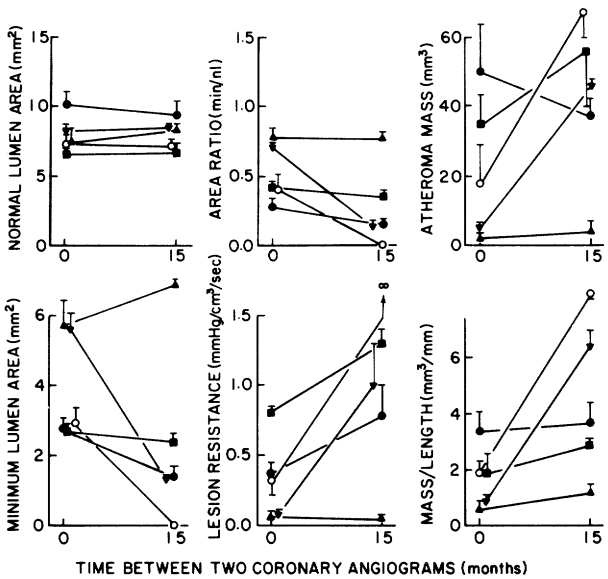

FIGURE 6. *Interval changes in computed parameters in five lesions over a period of 15 months in a patient with progressive anginal symptoms. Progression could be documented in at least three of the five nonocclusive lesions present at the first study, including one which progressed to complete obstruction. There was no significant progression in the lesion length, or of the diameter of the "normal" proximal and distal portions of the vessel. The range indicates the standard deviation from the mean of three separate estimates made from frame pairs spaced equally through the cardiac cycle.*

Discussion

We feel that this method facilitates an objective, repeatable approach to the analysis of arterial disease. It employs straightforward geometric principles to reconstruct a three-dimensional characterization of the vessel lumen from good quality angiograms. These paired, perpendicular angiographic views are not filmed simultaneously (biplane). Instead, frame pairs are selected from different coronary injections, but from the same point in the cardiac cycle (e.g., end systole, end diastole, mid-cycle). Identification of these frames is relatively simple. Although the known coronary elastic modulus[22] excludes detectable lumen diameter change during the arterial pulse, selection of synchronized frame pairs is necessary to avoid errors caused by axial and spatial rotation of the segment during the cardiac cycle.

The method assumes an elliptical vessel cross-section, with major and minor axes equal to the longer and shorter of the two diameters determined by the computer. Based on our observations with pressure-injected postmortem human arteries, this assumption appears reasonable. There are several errors inherent in the method. If the axes of the two projections are not coincident with the true major and minor axes of the elliptical vessel lumen, estimates of cross-sectional area will have a maximum error of the order $(\epsilon + 1/\epsilon - 2)/4$, where ϵ is the elliptical major-to-minor axis ratio. For $\epsilon = 1.5$, this amounts to 4%. Errors arise when the chosen vessel segment approaches a horizontal orientation (perpendicular to the y-axis) in either of the two projections. In practical terms, this reflects the problem of viewing the vessel segment end-on. There are *three* such sources of error which we call "horizontal axis ambiguities:" 1) Portions of the vessel may overlap the stenosis to obscure its detail. This "overlapping shoulder" effect does not appear to be a problem unless the lesion axis is less than 25° from the horizontal. 2) The diameters (dr, dl) determined from the two perpendicular angiographic views are perpendicular to each other *in the vessel cross-section* only when the local centerline axis is vertical in at least one of the two angiographic views. Maximum errors in area estimation of the order $(\epsilon\text{-}1) \cos \theta_R \cos \theta_L$ occur in the nonvertical situation. θ_R and θ_L are the angles of the vessel axis from the horizontal in the two angiographic views. Thus, for $\epsilon = 1.4$, and θ_R and θ_L greater than 30°, errors in area should be no greater than 10%, usually much smaller. 3) When the centerline of the vessel segment passes through horizontal, expression 6 becomes indeterminate, since the centerline coordinates are no longer a unique function of yi, the matching variable. These "horizontal axis ambiguities" are common to the proximal left anterior descending and posterior descending arteries, which tend to be viewed end-on in the LAO projections and to the left main and mid-LCCAs in the RAO. Modified projections, such as the LAO half-axial, can be used to minimize this problem. As an alternative, the program has the capacity for single projection analysis in which a circular lumen cross-section is assumed. This introduces a maximum error of the order $(\epsilon\text{-}1)$ on area estimations. While errors of this magnitude may be unacceptably large, estimates of *change* made from analysis of serial views made in the *same* single projection are likely to be valid.

The technique of matching the two views at points of minimum local lumen diameter is another potential source of error, even with circumspect editing to avoid obvious mismatches. It is based on the entirely arbitrary and untested assumption that a localized constriction occurs at the same point in the vessel in both angiographic views. There are a variety of potential methods for matching views; it remains to be determined which is the most effective.

Obviously not all coronary lesions can be analyzed by this technique. Factors which exclude a lesion from analysis are: 1) poor image quality, 2) obscuring of a lesion by an overlapping vessel, 3) horizontal orientation of the centerline axis which the computer will not tolerate in the paired analysis mode, and 4) end-on viewing. However, with careful attention to filming technique and film processing,[23] and with adequate numbers of projection pairs (including half-axial views), 60% to 70% of all lesions may be analyzed. By using single projection analysis when necessary, up to 90% of lesions can be measured.

The time cost of improved accuracy is considerable. For the average lesion, we now spend 6–8 minutes in frame pair selection, 4–6 minutes in tracing, and 8 minutes in digitizing and computer processing. Thus the method is clearly a research tool of limited clinical utility in its present form.

The two clinical examples illustrate the use of this method in three of the most active areas of coronary disease investigation: vasospasm, drug effects, and progression of atherosclerosis. The observations in the patient with Prinzmetal's angina suggest that diffuse vasospasm is the overlying pathophysiologic mechanism, but that underlying atherosclerotic disease can strikingly enhance the focal hemodynamic effects of spasm, as the plaque is squeezed into the vessel lumen.

This technique may find its greatest usefulness in evaluating the progression of atherosclerosis. Currently, the

most widely used assessment of lesion magnitude is a visual estimate of percentage diameter reduction, relative to a "normal" nearby portion of the vessel. The errors inherent in this type of analysis are widely accepted: 1) Individual observers may vary considerably in their assessment.[3] Bemis et al.[24] accepted only 20% or greater changes in visual estimates of lumen constriction as significant in serial coronary angiography. From personal experience, even greater interobserver variation among well-qualified diagnostic cardiologists and radiologists is not uncommon. 2) Estimates of percent stenosis, particularly if based on a single view, provide little objective information about the absolute dimensions or the hemodynamic consequences of the lesion. Frequently the "normal" vessel which forms the denominator of the "% stenosis" estimate is itself diffusely narrowed. On the other hand, using clinical arteriograms and a computerized analysis, it would appear that trained observers can measure vessel dimensions, in absolute, with a standard deviation of approximately 100–150 microns. Since typical vessels are of the order of 3 mm diameter, the standard deviation of the dimensional estimate is of the order of ± 3–5% of the lumen. This represents a significant improvement over the accuracy previously available. Furthermore, the computer can perform searches and tedious calculations to estimate other potentially important parameters of lesion severity. In particular, estimates of minimum cross-sectional area appear to provide a sensitive means of determining progression of an atherosclerotic lesion. The computed Poiseuille resistance represents an integrated average of a function of lumen constriction, weighted by the nature of the function toward the most severely constricted portion of the lesion; it appears to provide an even more sensitive index of disease progression than diameter or area estimations alone. Resistance is also (in theory) a more relevant index of the physiologic severity of the arterial stenosis.

Acknowledgment

We wish to thank Drs. Melvin Figley and John Murray for their inspiration and editorial comments, and Dr. Dennis Reichenbach, who performed the histopathologic measurements. Dr. Merri McMahon, Dr. Simeon Rubenstein, and Ms. Carol Ross assisted with the variability analysis. Mrs. Lacy Goede prepared the manuscript.

References

1. Robbins SL, Rodriguez FL, Wragg AL, Fish SJ: Problems in the quantitation of coronary atherosclerosis. Am J Cardiol **18:** 153, 1966
2. Robbins SL, Fish JJ: A new angiographic technique providing a simultaneous permanent cast of the coronary lumen. Am J Clin Path **42:** 156, 1964
3. Detre KM, Wright E, Murphy ML, Takaro T: Observer agreement in evaluating coronary angiograms. Circulation **52:** 979, 1975
4. Blankenhorn DH, Brooks SH, Seltzer RH, Crawford DW, Chin HP: Assessment of atherosclerosis from angiographic images. Proc Soc Exp Biol Med **145:** 1298, 1974
5. Crawford DW, Beckenbach ES, Blankenhorn DH, Seltzer RH, Brooks SH: Grading of coronary atherosclerosis: Comparison of a modified IAP visual grading method and a new quantitative angiographic technique. Atherosclerosis **19:** 231, 1974
6. Gensini GG, Kelly AE, Da Costa BCB, Huntington PP: Quantitative angiography: The measurement of coronary vasomobility in the intact animal and man. Chest **60:** 522, 1971
7. Chilvers AS, Thomas ML, Browse NL: The progression of atherosclerosis: A radiological study. Circulation **50:** 402, 1974
8. May AG, Deweese JA, Rob CG: Hemodynamic effects of arterial stenosis. Surgery **53:** 513, 1963
9. Yellin A: The laminar-turbulent transition in pulsatile flow. Circ Res **19:** 791, 1966
10. Young DF, Cholvin NR, Roth AC: Pressure drop across artificially induced stenosis in femoral arteries of dogs. Circ Res **36:** 735, 1975
11. Young DF, Tsai FY: Flow characteristics in models of arterial stenosis. I. Steady flow. J Biomech **6:** 395, 1973
12. Young DF, Tsai FY: Flow characteristics in models of arterial stenosis. II. Unsteady flow. J Biomech **6:** 547, 1973
13. Gould KL, Lipscomb K: Effects of coronary stenosis on coronary flow reserve and resistance. Am J Cardiol **34:** 48, 1974
14. Gould KL, Lipscomb K, Calvert D: Compensatory changes of the distal coronary vascular bed during progressive coronary constriction. Circulation **51:** 1085, 1975
15. Logan SE: On the fluid mechanics of human coronary artery stenosis. IEEE Trans BME BME-**22:** 327, 1975
16. Jaffee R, Glancy DL, Epstein SE, Brown BG, Morrow AG: Coronary arterial-right heart fistula. Long term observations in seven patients. Circulation **48:** 133, 1973
17. Schlichting HR: Boundary Layer Theory, ed 4. New York, McGraw Hill, 1962, p 502
18. Chaturvedi MC: Flow characteristics of axisymmetric expansions. Proc Am Soc Civil Engrs **89:** Hy3, 61, 1963
19. Chien S, Usami RJ, Dellenback MI, Gregersen MI: Blood viscosity: Influence of erythrocyte deformation. Science **157:** 827, 1967
20. Schlesinger MJ: New radiopaque mass for vascular injection. Lab Invest **6:** 1, 1957
21. Prinzmetal M, Kennamer R, Merliss R, Wada T, Bor N: Angina pectoris. I. A variant form of angina pectoris. Am J Med **27:** 375, 1959
22. Patel DJ, Janicki JS: Static elastic properties of the left coronary circumflex artery and the common carotid artery in dogs. Circ Res **27:** 149, 1970
23. Kato W, Wong M: Optimizing cine film. Cath Cardiovasc Diag **1:** 97, 1975
24. Bemis CE, Gorlin R, Kemp HG, Herman MV: Progression of coronary artery disease. A clinical arteriographic study. Circulation **47:** 455, 1973